Extended abstract for PPS07ea, Gothenburg, Sweden, August 2007

Mechanical response of injection-moulded parts at high strain rates

T. Glomsaker[a], E. Andreassen[a], M. Polanco-Loria[b], O. V. Lyngstad[c], R. H. Gaarder[a], E. L. Hinrichsen[a]

[a] SINTEF Materials and Chemistry, Oslo, Norway
[b] SINTEF Materials and Chemistry, Trondheim, Norway
[c] Plastal AS, Raufoss, Norway

e-mail: erik.andreassen@sintef.no

INTRODUCTION

This paper deals with numerical simulation of the impact response of injection-moulded parts, and the mechanical testing associated with this. The automotive industry is a driving force in this field, and a standard for obtaining tensile properties at high strain rates was recently published [1].

Some comments to justify this paper being presented at a conference on polymer processing: The anisotropy and inhomogeneity of injection-moulded parts is a challenge when trying to model and simulate their mechanical response at large strains. The goal is to simulate of the mechanical response with local mechanical parameters from a simulation of the moulding process, but this has so far only been demonstrated for simple geometries and/or small strains. Even for simple test specimens there are several questions: Is it OK to compare different materials, with e.g. different molecular weight, moulded with the same machine settings? Can we assume that specimens with different thicknesses (e.g. 2 mm and 4 mm) have the same effective morphology? How do differences in morphology, anisotropy etc interfere with the stress distribution? Does the skin layer affect the test results? How about residual stresses from the moulding process?

This paper presents experimental results, and simulated responses with different material models, based on a study with a mineral and elastomer modified polypropylene (PP) material. The main objective of the work was to investigate the validity of linear-elastic viscoplastic constitutive equations. A Mises type model and a pressure sensitive model were implemented in LS-DYNA. Model parameters were obtained by tensile testing over five decades of strain rate, as well as quasi-static compression. The model was then checked by simulating two tests: Three-point bending of beams and central loading of circular plates.

Numerical simulation of impact loading of polymer materials is of increasing interest as these materials are frequently applied in critical applications and constructions. In particular, the response to impact loads is of interest for automotive applications related to passenger and pedestrian safety where the material may undergo large multiaxial deformations at high strain rates. Also electronic casings and various ‘everyday’ products must be designed to resist impact loads. Various commercial simulation codes have suitable numerical techniques to simulate the dynamic event of an impact. However, most of the constitutive models in these codes were developed for metals and little work has been published in the literature in order to verify these models for polymer materials. Verification of a model for simulating impact should as a minimum include different stress states, e.g. bending and biaxial stress, at a range of different loading rates. Polymer materials used in components designed to withstand impact and/or absorb impact energy are usually highly ductile. Ductile polymeric materials show a complex behavior in impact loading involving large strains. The complexity applies to the micromechanical mechanisms as well as the macroscopic response.

In the literature on simulation of impact loading of solid polymers, early models were based on the traditional linear-elastic viscoplastic formulation with a von Mises based yield criterion and flow rule. With such models several authors concluded that quasi-static tensile tests at different strain rates are insufficient to determine the parameters for impact simulations. Duan et al. [2] applied a viscoplastic material model fitted to uniaxial compression tests at low strain rates, and included a pressure dependendent yield curve, and

material failure at a maximum plastic strain. They reported reasonable results for a falling weight test, but only for one speed. Pyttel and Weyer [3] applied a non-isothermal elastic-viscoplastic G'Sell model with a small initial yield stress to simulate impact on a honeycomb plate. They obtained reasonable simulations of impact on honeycomb plates at 4.0 and 5.3 m/s for both loading and unloading. Dean and Wright [4] applied an elastic-viscoplastic model with a linear Drucker-Prager yield criterion and a non-associative flow rule implying plastic dilatation. The viscoplastic model was fitted to experiments at a range of strain rates up to 100 s^{-1}. Simulations of a plate loaded at constant velocities between 0.1 mm/s and 1 m/s showed good correlation with experiments. Dean and Crocker [5,6] have also introduced a new model taking into account the effect of cavitation on the plastic deformation. Finally, the model of Du Bois et al. [7,8] must be mentioned. The aim of this model, the *semi-analytical model for polymers with C^1-differentiable yield surface* (SAMP-1), is to 'include all relevant experimentally observed effects in one model'.

MODELLING

Summary of the material model

The model used in this study can be summarised as follows:

- A linear-elastic–viscoplastic model with pressure sensitivity and plastic dilatation.
- For the elastic response, non-linearity and rate effects are neglected.
- 'Viscoplastic' means rate dependent yield stress and plastic flow.
- The Raghava yield criterion [9] was used. This is a modification of the von Mises criterion, and it accounts for yielding being sensitive to the hydrostatic stress (pressure), giving different yield stresses in tension and compression. A part of the molecular basis for this can be that the chains are disentangled in tension, but not in compression.
- The flow rule (plastic strain vs stress) was obtained from a Drucker-Prager flow potential. This flow rule accounts for volume change (dilatation) during plastic flow. The plastic dilatation observed for polymers is due to cavitation/crazing (for shear yielding the volume is constant).
- This linear-elastic–viscoplastic model was implemented in LS-DYNA as a modification of the material model MAT24 (*piecewise linear plasticity*).

Yield criterion

The initial yielding of a wide range of crystalline and amorphous polymers can be described by the Raghava criterion [9]. This criterion, which is a modification of the von Mises criterion, accounts for different yield stresses in tension and compression. Yielding not only depends on the shear stress (as in the von Mises criterion), but also on the hydrostatic stress:

$$(\sigma_1-\sigma_2)^2+(\sigma_2-\sigma_3)^2+(\sigma_3-\sigma_1)^2+2(\sigma_C-\sigma_T)(\sigma_1+\sigma_2+\sigma_3)=2\sigma_C\sigma_T \quad \textbf{(1)}$$

Here,

- σ_1, σ_2 and σ_3 are the principal stresses
- σ_C and σ_T are the yield stresses in tension and compression (note that the von Mises equation is recovered when setting $\sigma_C = \sigma_T$).

Introducing

- $\lambda = \sigma_C / \sigma_T$, the pressure sensitivity parameter
- J_2, the second deviatoric stress invariant
- I_1, the first stress invariant

Eq. (**1**) can be rewritten as:

$$3J_2 + (\lambda - 1)\sigma_T I_1 = \lambda \sigma_T^2 \qquad \textbf{(2)}$$

Furthermore, Eq. (**2**) can be rewritten in a classical form $\sigma_{eq}^R = \sigma_T(\varepsilon_{eq}^P)$, as:

$$\sigma_{eq}^R = \frac{(\lambda - 1)I_1 + \sqrt{(\lambda - 1)^2 I_1^2 + 12\lambda J_2}}{2\lambda} = \sigma_T(\varepsilon_{eq}^P) \qquad \textbf{(3)}$$

In this definition,

- σ_{eq}^R represents the equivalent stress in the Raghava sense
- $\sigma_T(\varepsilon_{eq}^P)$ represents the softening/hardening function which can be generalised using a tabular form of true stress vs. true plastic strain values.

Thus, this yield criterion requires two main inputs: The uniaxial stress-strain curve (in tension) and the pressure sensitivity parameter λ .

Flow rule

In the elastic-plastic framework, a flow rule is used for the determination of plastic strains. The components of the plastic strain tensor are assumed to be proportional to the derivative of a potential function *G* with respect to the components of the stress tensor. In this work, we use a non-associative linear Drucker-Prager model as the flow potential, as proposed by Dean and Wright [4]. The potential function can be expressed as

$$G(I_1, J_2) = \sqrt{3J_2} + \alpha\, I_1/3 \qquad \textbf{(4)}$$

Here, α is a material parameter that we will return to below. The plastic strain tensor can then be calculated as:

$$d\varepsilon_{ij}^p = d\xi \frac{\partial G}{\partial \sigma_{ij}} = d\xi \left[\frac{\sqrt{3}}{2} \frac{S_{ij}}{\sqrt{J_2}} + \frac{\alpha\, \delta_{ij}}{3} \right] \qquad \textbf{(5)}$$

Here

- $d\varepsilon_{ij}^p$ is the incremental plastic strain tensor
- $d\xi$ is the plastic multiplier
- σ_{ij} is the stress tensor
- S_{ij} is the deviatoric stress tensor
- δ_{ij} is the Kronecker delta function
- α is a material parameter defined as the the volumetric plastic strain divided by the equivalent von Mises plastic strain

For uniaxial tension, α can be related to the 'plastic' Poisson's ratio ν_p (the ratio between the transversal and longitudinal plastic strains, for large strains):

$$\alpha = \frac{3(1 - 2\nu_p)}{2(1 + \nu_p)} \qquad (6)$$

DETERMINATION OF MATERIAL PARAMETERS

Material

The material used in this study was a mineral and elastomer modified polypropylene (PP) compound provided by Borealis. The density was 940 kg/m^3 and the melt flow rate (230°C/2.16kg) was 17 g/10 min. This material is typically used in injection-molded automotive applications. Recently three more materials were tested and simulated as described below, but this paper will focus on the PP material mentioned above.

Uniaxial tensile testing

Uniaxial tensile testing was conducted at a range of different strain rates using standard injection-moulded test specimens (type 1A of ISO 527-2) with cross-section 4 mm × 10 mm. The crosshead speeds ranged from 5 mm/min (8.33 x 10^{-5} m/s) to 5 m/s. For crosshead speeds up to 500 mm/min a *Zwick Z250* machine was used, and the elongation was measured with a conventional extensiometer. At higher rates a modified *Schenk/Instron VHS* was used, and the elongation was taken as the displacement of the crosshead. Fig. 1 shows the nominal stress-strain data, as defined by

$$\sigma_n = \frac{F}{A_0} \qquad \varepsilon_n = \frac{\Delta L}{L_0} \tag{7}$$

where

- F is the measured force
- A_0 is the initial cross-section of the specimen (prior to loading)
- ΔL is the elongation of the specimen
- L_0 is the initial length of the specimen

At 5 m/s some oscillations appeared in the recorded force, which we attribute to resonance of the instrument. Fig. 1 shows that the stress level increases with the loading rate. The rate sensitivity of the yield stress, as well as post-yield stress at a given nominal strain, can be represented by an Eyring equation:

$$\sigma = A_0 \ln \dot{\varepsilon} + A_1 \tag{8}$$

Some necking was observed. Hence, video recording and image analysis was used to calculate true stress-strain curves and plastic Poisson's ratios. At quasi-static conditions a camera with resolution 1024 × 1024 pixels and recording rate 40 frames per second (fps) was used, while a 8000 fps camera was used at high strain rates (not reported in this paper). The specimens were black and they were marked with white stripes for the video recording and image analysis. From the image analysis, the longitudinal (axial) strains, and the transversal strains in the width direction, were determined. The transversal strain in the thickness direction was assumed to be similar to that in the width direction (this was checked for some specimens with a conventional extensiometer). Hence, true stresses and plastic Poisson's ratios could be determined with the following equations:

$$\sigma = \frac{FW_0}{W^2 H_0} \tag{9}$$

$$\nu_p = -\frac{\varepsilon_p^T}{\varepsilon_p^L} \tag{10}$$

where

- F is the measured force
- W_0 is the initial width of the specimen
- W is the measured width during testing

- H_0 is the initial thickness of the specimen
- ε_p^T and ε_p^L are the true transversal and longitudinal plastic strains

Fig. 2 shows the 'standard' true stress-strain, assuming homogenous deformation and constant volume in plastic deformation (i.e. assuming a plastic Poisson's ratio equal to 0.5), and the true stress-strain as determined by video image analysis. There are significant differences. Fig. 2 also shows the calculated plastic Poisson's ratio based on Eq. (**10**). The value decreases with strain, starting at ~0.3 at 20% strain. However, the Drucker-Prager model in Eqs. (**4**)-(**6**) considers a constant plastic Poisson's ratio. Therefore, an effective plastic Poisson's ratio was defined, so that the true stress-strain calculated with this (constant) effective plastic Poisson's ratio agreed with the stress-strain determined with the video extensiometer. As shown in Fig. 2, using a plastic Poisson's ratio of 0.25 gave a reasonable agreement. However, there was a deviation at small strains, which was caused by the relatively coarse resolution of the video camera. Therefore, the actual flow curve used in simulations was based on strains measured with the conventional extensiometer for small strains, and strains from the video measurements at larger strains.

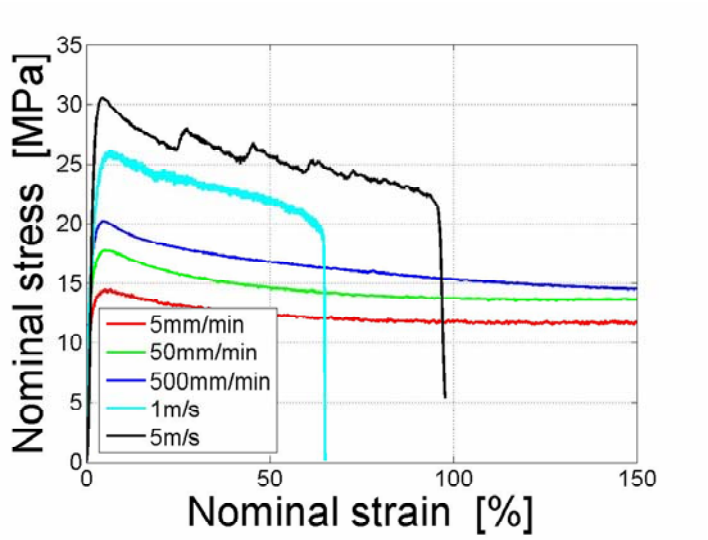

Figure 1 Nominal tensile stress versus nominal tensile strain with different crosshead speeds.

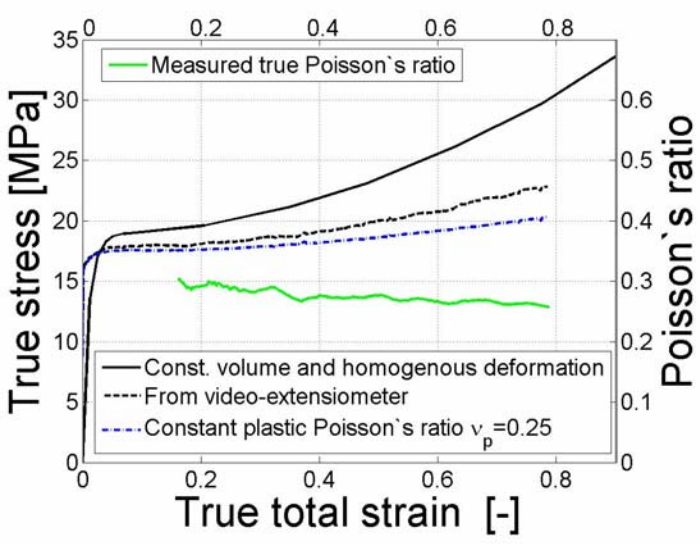

Figure 2 Measured true stress-strain and Poisson's ratio at a nominal strain rate of 9.3 x 10^{-3} s^{-1}. See main text for details.

In the simulations, the flow curve in Fig. 2 was scaled to a nominal strain rate of 9.3 x 10^{-4} s^{-1} using the Eyring parameters, and this reference curve was then given as data points to LS-DYNA which interpolated for strains between the individual points, and scaled the stress with the strain rate according to the Eyring equation

$$\sigma(\varepsilon, \dot{\varepsilon}) = \sigma_0(\varepsilon)\left[B_0 \ln \dot{\varepsilon} + B_1\right] \quad \textbf{(11)}$$

where $\sigma_0(\varepsilon)$ is the reference flow curve at the nominal strain rate of 9.3 x 10^{-4} s^{-1}.

Uniaxial compression

Finally, compression tests based on ISO 604 were conducted using specimens milled from the injection moulded multipurpose specimens. The specimens used in the compression tests were 10 mm high (loading direction) with a cross-section of 4 mm x 10 mm. Nominal stress strain curves for two different crosshead speeds are shown in Fig. 3, together with tensile data scaled to the same nominal strain rates. As expected, a higher yield stress is observed in the compression test. There are various methods to extract the pressure sensitivity parameter λ from these experiments, but as a first approximation one may apply the ratio of the yield points (i.e. the maximum nominal stresses). This gives a pressure sensitivity λ = 1.35. The nominal stress-strain curves for compression and tension show similar strain hardening, except that the yield point in compression appears at a higher strain than in tension. At high strains – typically above ~25% – the specimens start buckling.

In order to assess the compression test, injection-moulded specimens of two more PP grades (compounds for the automotive market) were tested. Also compression-moulded specimens with different cross-sections (same height of 10 mm) were tested. The three PP grades had quite similar stress-strain curves (Fig. 4). Compression-moulded specimens (Fig. 5) showed more pronounced strain hardening than injection-moulded specimens. The different cross-sections of the compression-moulded specimens gave similar stress-strain curves, but the differences were experimentally significant (Fig. 5).

Material parameters

The actual input parameters to the model are given in Table 1. Additionally, some of the tests to be simulated involved friction between the polymer and steel tools. For simplicity, Colomb friction was assumed, and the static and dynamic friction coefficients were set to the same value. The values used are mentioned for the respective cases in the next section.

Table 1 Material parameters used in the simulations.

Young's modulus E	2500 MPa
Elastic Poisson's ratio ν	0.4 [-]
Initial yield stress σ_{y0}	2 MPa
Density ρ	940 kg/m^3
Plastic Poisson's ratio ν_p	0.25 [-]
Strain rate sensitivity B_0	0.0954 [-]
Strain rate sensitivity B_1	1.67 [-]
Pressure sensitivity λ	1.35 [-]

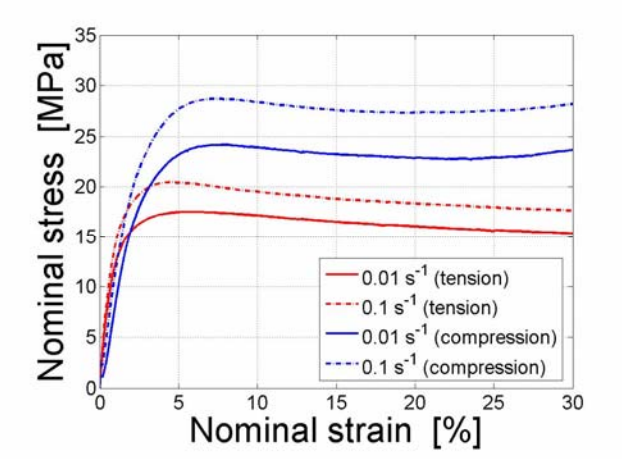

Figure 3 Stress-strain curves for compression and tension at the same strain rates.

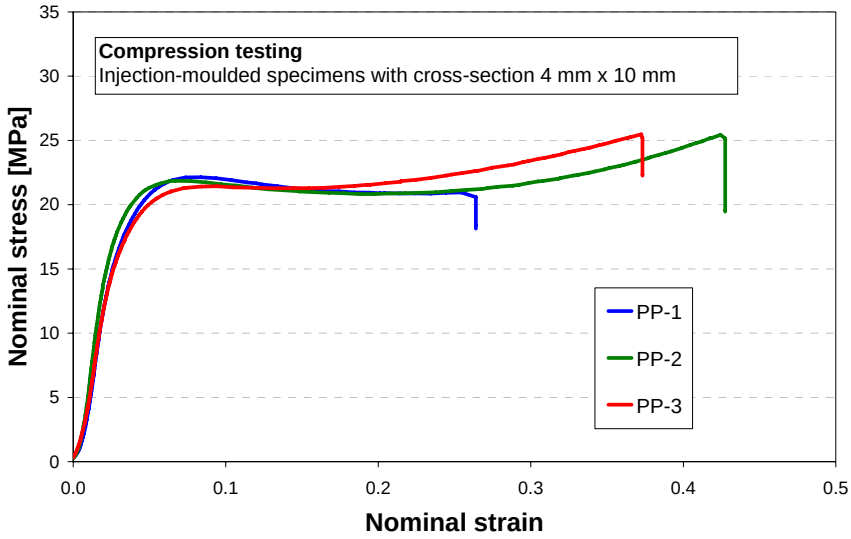

Figure 4 Data from compression testing of three PP materials (PP-1 is the main material in this paper). Injection-moulded specimens with cross-section 4 x 10 mm^2. Nominal strain rate 3.3 x 10^{-3} s^{-1}. End of test is arbitrary (but always above a strain of 0.2).

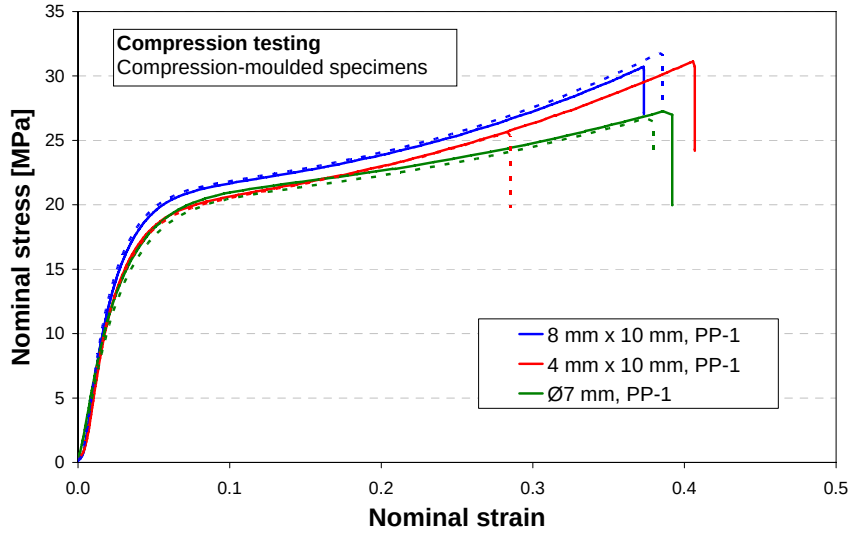

Figure 5 Data from compression testing of compress-moulded specimens with different cross-sections as indicated in the legend. Nominal strain rate 3.3 x 10^{-3} s^{-1}. Test parallels are indicated by dotted lines (same colour for same cross-section). End of test is arbitrary (but always above a strain of 0.2).

SIMULATIONS VS. EXPERIMENTS

The tests listed below (FEM meshes shown in Fig. 6) were simulated and compared to experiments:

- Tensile testing at strain rates up to 5 m/s
- Compression testing (quasi-static)
- Three-point bending at speeds up to 4 m/s
- Centrally loaded circular plate (biaxial loading), at speeds up to 4 m/s

<table>
<tr>
<td> 
Uniaxial tensile testing.
Cross-section of specimen: 4 mm x 10 mm.</td>
<td> 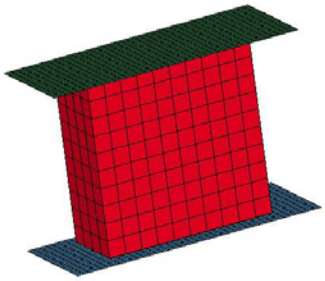
Uniaxial compression testing. Specimen height: 10 mm. Specimen cross-section: 4 mm x 10 mm</td>
</tr>
<tr>
<td> 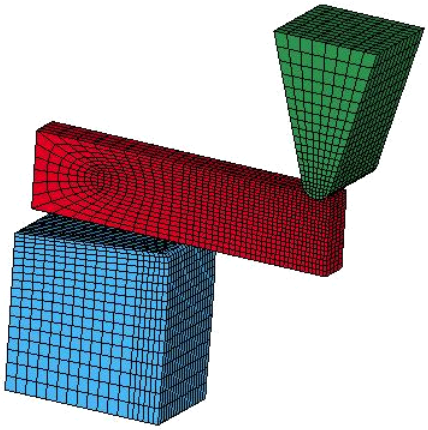
Three-point bending. Only one half of the specimen (red) and one of the supports (blue) are shown). Specimen cross-section: 4 mm x 10 mm. Distance between supports: 40 mm.</td>
<td> 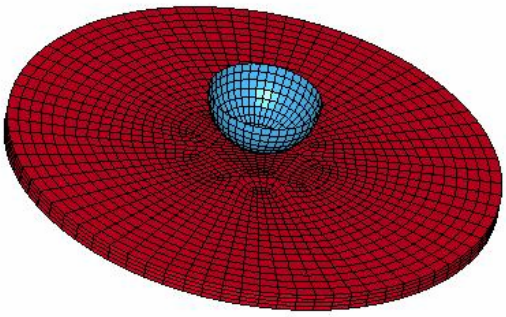
Centrally loaded plate with thickness 2 mm and diameter 60 mm. Both freely supported and clamped plates were tested, see main text.</td>
</tr>
</table>

Figure 6 Geometries and meshes for the tests.

Uniaxial tension: Simulations of the tensile tests, using the parameters in Table 1, are shown in Fig. 7. As one should expect, there is a good agreement between simulations and experiments. Similar good correlation was also obtained with a von Mises type model – i.e. with a plastic Poisson's ratio of 0.5 and no pressure dependence. However, in the experiments there was a slight necking, which was more pronounced at high strain rates, while the simulations showed uniform deformation.

Uniaxial compression: The compression tests were simulated using a Colomb friction factor of 0.25. Only the initial behavior was well predicted. Beyond the yield point the simulations (based on the flow curve in tension) overpredicted the strain hardening.

Three-point bending: Beams were subjected to three-point bending using a Charpy fixture as indicated in Fig. 6. In the simulations the friction coefficient was set to 0.15. Tests were conducted at a range of velocities from 5 mm/min to 4 m/s. For tests with loading rates up to 500 mm/min a constant rate was maintained during the experiment. At higher loading rates a free-falling impactor (mass 3.15 kg) equipped with a piezo-electric load cell was used. Fig. 8 shows experimental and simulated force versus displacement. The standard von Mises elastic-viscoplastic assumptions (a plastic Poisson's ratio of 0.5 and no pressure dependence) gave a better prediction than the modified model for this case, and it is the simulations with the von Mises model that are shown in Fig. 8. The reason why the modified model is inferior is probably due to the compressive stresses being overestimated, as mentioned above. Some of the deformed specimens are shown in Fig. 9. At 4 m/s the beam was squeezed down between the supports.

Centrally loaded circular plate: These 2 mm thick plates were loaded at rates between 5 mm/min and 4 m/s. Tests with loading rates below 500 mm/min were conducted with constant crosshead speed and the plate was freely supported. At higher loading rates, the tests were conducted with an instrumented free-falling impactor (the same as used for the three-point bending) on a clamped plate. Fig. 10 shows the experimental and simulated force versus displacement for the highest loading rates. The simulations in Fig. 10 are based on the pressure sensitive model (Table 1) which for this case is slightly better than the model based on von Mises. Fig. 11 shows the deformed plates after testing. Note that the plate was perforated when the impactor had a speed of 4 m/s (impactor mass 3.15 kg), ref. the solid blue curve in Fig. 10. For the impact speeds 0.7 m/s and 1 m/s the force curves are overpredicted, and the unloading occurs to early.and overpredicted at the two highest impact rates. the unloading stage. For the impact speeds 2 m/s and 4 m/s the predictions are OK up to half the maximum force. After this the force is overpredicted. Again the unloading is not predicted, but this could not be expected with the present model.

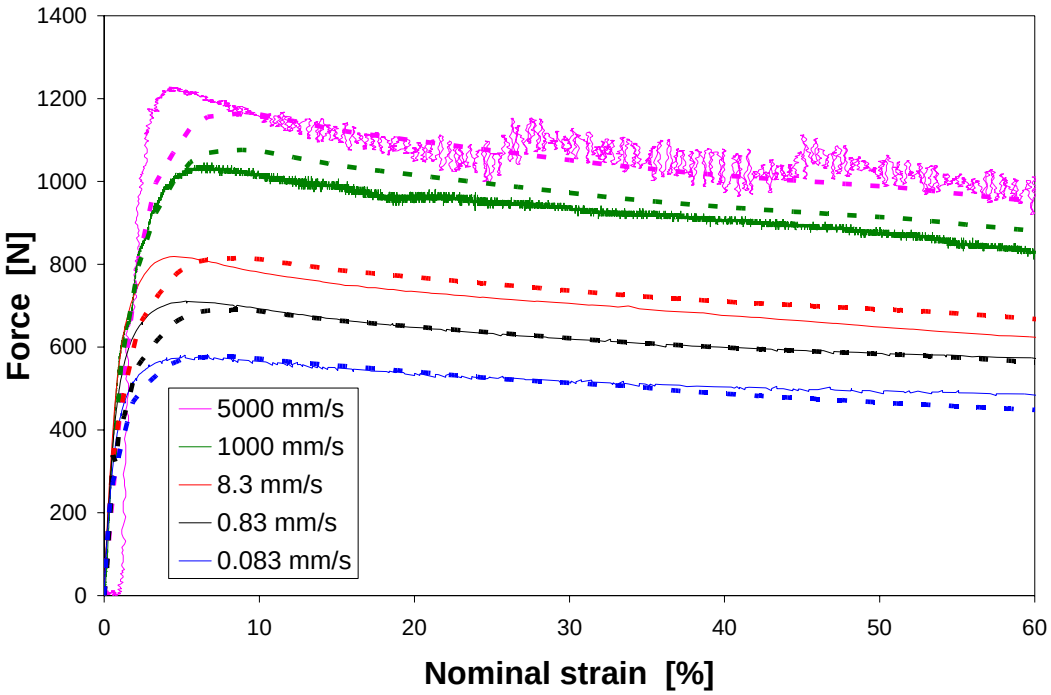

Figure 7 Tensile testing: Experimental data (solid lines) and simulated response (dashed lines) with parameters given in Table 1. Crosshead speeds as given in the legend.

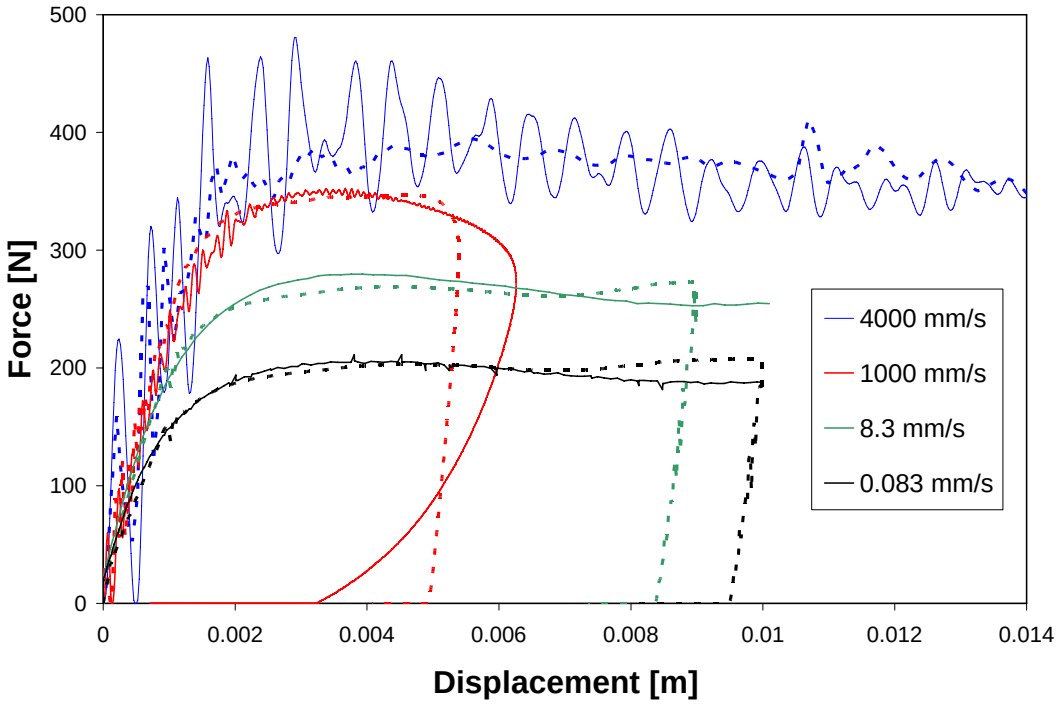

Figure 8 Force vs. displacement for three-point bending. Experimental results (solid lines) and simulations (dashed lines) using a von Mises based model. Loading rates in legend.

4 m/s (free-falling impactor)

1 m/s (free-falling impactor)

500 mm/min (constant speed)

Figure 9 Deformed specimens after three-point bending tests at different loading rates.

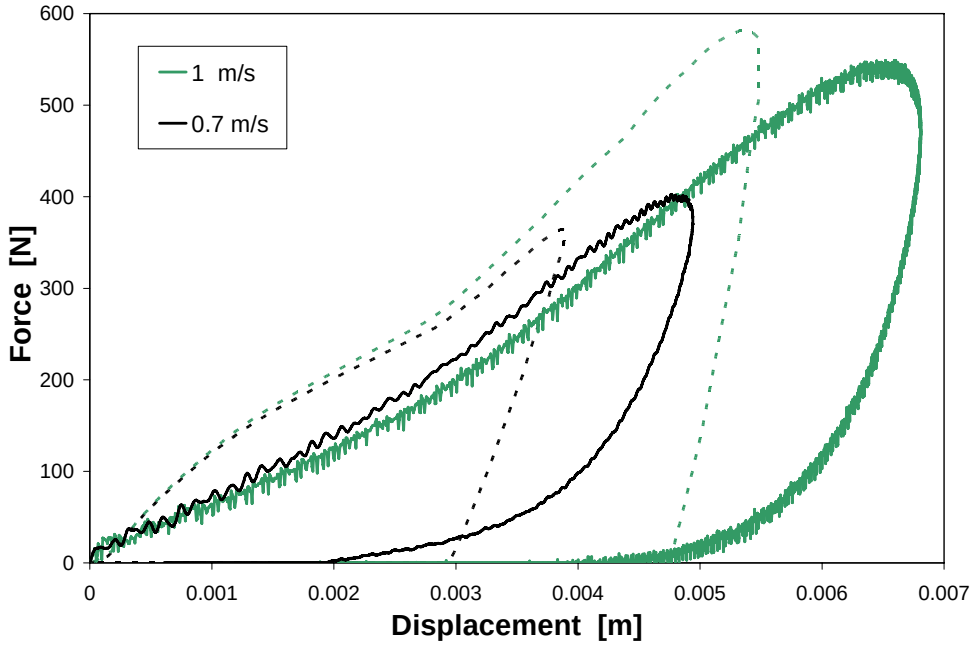

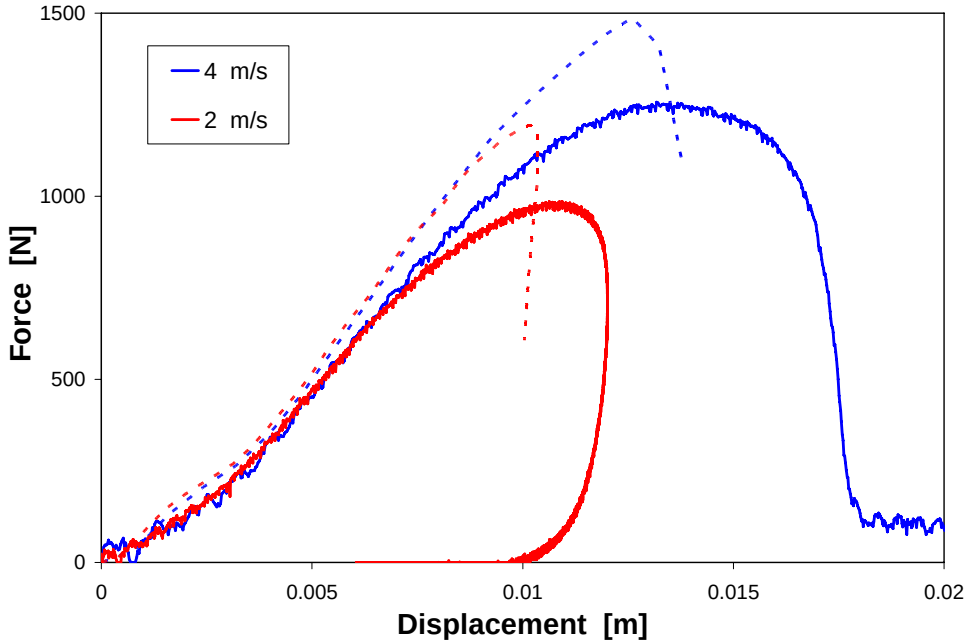

Figure 10 Impact force vs. displacement for centrally loaded plate. Experimental results (solid lines) and simulations (dashed lines) using the model with parameters in Table 1. Impact speeds in legend.

Figure 11 Deformed plates after testing with impact rates 1, 2 and 4 m/s (left to right).

DISCUSSION

The results reported in this paper are preliminary. There are room for improvements, in particular when it comes to the input parameters (testing and analysis). Also, only results for one material is reported. Work in progress considers additional materials (similar PP grades)

The loading and unloading phases must be discussed separately. During loading, the simulations with both the von Mises based model and the pressure sensitive model showed reasonable good agreement with the measurements, for both the three-point bending and the centrally loaded plate, at different loading rates. However, the pressure sensitive model was not overall significantly more accurate than the von Mises based model. In fact, for the three-point bending the latter model was slightly better. The reason for this may be systematic and/or non-systematic experimental errors (like non-ideal stress distributions, friction and adiabatic heating), as well as insufficiencies in the constitutive formulation. We have found that simulation of uniaxial compression, with both the von Mises based model and the pressure sensitive model, overpredicts the stresses at large strains. Also, the rate effects are slightly different in tension and compression. The pressure sensitive model amplifies the overprediction of compressive stresses, and this may be the reason why the von Mises based model appeared to be better than the pressure sensitive model in simulation of bending. Furthermore, in the simulations of the centrally loaded plate, the pressure sensitive model gave some stiffness reduction compared to the von Mises based model, due to the plastic dilatation effect. (Just as for a linear-elastic plate where reduction in the Poisson's number reduces the stiffness.) Also, because the plate is dominated by membrane stresses, the possible shortcomings of the pressure sensitive model in compression have less effect.

Concerning the unloading phase there is poor agreement with measurements for both models, as could be expected with linear-elastic models. In particular, we note that the recoverable strains are much larger than predicted. This was also observed in the uniaxial tensile tests where it was found that the recoverable elastic strains after fracture were large, especially at high loading rates. Typically the recoverable strain was 40% of the total strain at fracture and one or two decades larger than the predicted linear-elastic strain. Thus, it is clear that a non-linear viscoelastic model should be considered. However, a simpler and pragmatic approach, considering reduction of the elastic modulus with increasing strain (damage), has been suggested by Du Bois et al. [8].

For many systems of practical interest it will also be highly interesting to be able to simulate the failure of the material/component. It is expected that a failure model may be complicated and it should probably include the deformation history of the material in some way to be generally valid. A constitutive equation reflecting the real physical behavior of the deformation in a more realistic way is probably necessary – supporting the need for a viscoelastic constitutive model.

CONCLUSION

It has been shown that mechanical loading of a thermoplastic material like polypropylene at large strains and different loadings rate may be reasonably well simulated by use of a linear-elastic viscoplastic constitutive equation of von Mises type. However, it is clear that these materials deviate from the von Mises model, since their yield stress increases with hydrostatic pressure and plastic dilatation occurs in tension. Therefore a modified model with these properties was implemented in LS-DYNA. Simulations with this modified model resulted in improved agreement between simulations and measurements for impact on a plate due to lower stiffness. For three-point bending the agreement was poorer, possibly due to different strain hardening in compression and tension. In the unloading stage, however, it is clear that the recoverable strain is non-linear and at least one decade larger than predicted by the linear elastic model.

ACKNOWLEDGEMENTS

Kristin Kaspersen at SINTEF is acknowledged for assistance with the video recording and Reinhard Bardenheier at Instron is acknowledged for assistance with the high-speed tensile testing equipment.

REFERENCES

[1] ISO 18872:2007 'Plastics – Determination of tensile properties at high strain rates'

[2] Duan Y., Saigal A., Greif R., Zimmerman M.A., *Polym. Eng. Sci*., 42, 395 (2002)

[3] Pyttel T. and Weyer S., *Int. J. Crashworthiness*, 8, 433 (2003).

[4] Dean G. and Wright L., *Polym. Testing*, 22, 625 (2003)

[5] Dean G. and Crocker L., *Plast. Rubber Composites*, 36, 1 (2007)

[6] Crocker L. and Dean G., *Plast. Rubber Composites*, 36, 14 (2007)

[7] Kolling S., Haufe A., Feucht M., Du Bois P.A., *4th German LS-DYNA Users' Conference*, Bamberg, Germany, 2005, pp. A-II-27 to A-II-52

[8] Du Bois, P.A., Kolling S., Koesters M., Frank T., *Int. J. Impact Eng*., 32, 725 (2006)

[9] Raghava R.S., Caddell R.M., Yeh G.S.Y., *J. Mater. Sci.*, 8, 225 (1973)